

Comparison among different software for the evaluation of moment-curvature of R.C. columns

Rosario Montuori^a, Elide Nastri^{*}, Maria Ilenia Palese^b and Vincenzo Piluso^c

Department of Civil Engineering, University of Salerno, Italy

(Received February 28, 2019, Revised April 29, 2019, Accepted July 20, 2019)

Abstract. The work aims at the comparison among commonly used research programs concerning moment-curvature ($M-\chi$) diagrams of confined R.C. members. The software considered in this work are Sap2000, SeismoStruct and Opensees. The curves provided by these software, given the same modelling, have been compared to those provided by a theoretical fiber model. A parametric analysis has been led on rectangular column sections with different level of axial load and different stirrups spacing. The accuracy of the modelling of the considered structural programs has been investigated by comparing their results with those obtained by applying the theoretical fiber model.

Keywords: confined concrete; reinforced concrete (RC); non-linear analysis; computer modeling; concrete constitutive models

1. Introduction

It has long been recognized that strength, as well as ductility of concrete, substantially increases whenever its state of stress is a triaxial compression. In practice, a loading condition equivalent to hydrostatic compression results when transverse reinforcement in the form of closed ties (hoops) or spirals, prevent lateral swelling of an element subjected to axial compression. The concrete which is affected by this favorable action of the transverse reinforcement is called confined concrete. It must be noted that some degree of confinement is contributed from longitudinal reinforcement bars, especially those of large diameter and/or with close spacing. The inelastic behavior of concrete is initiated by the formation of internal bond cracks at the interface between aggregates and mortar, a phenomenon which influences the descending branch of the stress (σ_c)-strain (ε_c) diagram. The behaviour of the material is affected by confinement from the instant that internal cracking causes an increase of volume in the element considered. It follows that transverse reinforcement does not affect the first part of the $\sigma_c-\varepsilon_c$ curve, but their contribution becomes significant as soon as the maximum strength is achieved.

Confinement offers two main advantages regarding the seismic behavior of concrete structural elements. In fact, it

increases the strength of concrete by compensating the spalling, i.e., the failure of the cover concrete, occurring when compressive strain in the cover exceed 0,4 % (Mander *et al.* 1988) and it reduces the slope of the descending branch of the $\sigma_c-\varepsilon_c$ curve. Therefore, it increases the maximum strain ε_{cu} leading to values higher than 0,35 %, commonly accepted by codes for members in bending, widely growing the local ductility of the members. The main parameters affecting the increase of ductility and strength are the ratio of transverse reinforcement (ρ_w), the yield strength of the transverse reinforcement (f_y) even if the increase of stress in the transverse reinforcement due to the strain hardening is typically ignored, the compressive strength of concrete (f_c), the spacing of transverse reinforcements (s) and the longitudinal bars pattern. Given this benefit, the confinement cannot be neglected both in the design of new building than in the evaluation of the seismic capacity of existing and aged R.C. buildings.

The first research on this topic was conducted by Richart *et al.* (1928), Balmer (1944). Afterwards, the issue of confinement has been the subject of many studies in which it has been pointed out that confinement is improved if 1) the transverse reinforcement is placed at relatively close spacing; 2) additional supplementary overlapping hoops or cross ties with several legs passing the section are included; 3) the longitudinal bars are well distributed around the perimeter; 4) the volume of transverse reinforcement to the volume of the concrete core or the yield strength of the transverse reinforcement is increased; 5) spirals or circular hoops are used instead of rectangular hoops and supplementary cross ties. These effects of confinement on the stress-strain behaviour of concrete have been quantified for the first time by Kent and Park (1971) for concrete confined by rectangular transverse reinforcement. The relationship proposed was based on the test results of Roy and Sozen (1964) and others available at

*Corresponding author, Ph.D.

E-mail: enastri@unisa.it

^aProfessor

E-mail: r.montuori@unisa.it

^bEngineering

E-mail: ileniapalese@gmail.com

^cProfessor

E-mail: v.piluso@unisa.it

that time. Anyway, this model neglects the increase in concrete strength but considers the increase in ductility due to rectangular confining steel rebars. Subsequently, Park *et al.* (1982), Scott *et al.* (1982) tested full-size specimens based on real building columns and modified the Kent and Park (1971) stress-strain relationship taking in account the enhancement of both the concrete strength and ductility due to confinement and the effect of strain rate. Other monotonic stress-strain equations for concrete confined by rectangular-shaped transverse reinforcement have been proposed by Vellenas *et al.* (1977), Sheikh and Uzumeri (1980, 1982). In particular, Sheikh and Uzumeri (1980, 1982) proposed a stress-strain model similar to the one proposed by Park *et al.* (1982). This model incorporates the confinement effects by adjusting the peak stress and setting a confinement effectiveness coefficient. The confinement effectiveness coefficient depends on the configuration of the hoop reinforcement. Stress-strain equations for concrete confined by spiral reinforcement have been proposed by Park and Leslie (1977), Desay *et al.* (1978), Ahmad and Shah (1982, 1985), Dilger *et al.* (1984), and others.

Mander, Priestley and Park (1988) proposed a unified stress-strain model for confined concrete, both for circular or rectangular sections, under static or dynamic loading, either monotonically or cycling applied. More recently, Mander and Chang (1994) developed a hysteretic model for confined and unconfined concrete subjected to both tensile and compressive cyclic loading. This concrete stress-strain model is a modern version of the well-known Mander, Priestley and Park (1988) model and has been enhanced to predict the behaviour of high strength concrete. The model is also capable of simulating gradual crack closure under cyclic loading. However, the monotonic part of the model is entirely coincident with the Mander, Priestley and Park model. Even if studies of Razvi (1999), Cusson *et al.* (1996), Cusson and Paultre (1995) and more recently of Dhakal and Maekawa (2002), Shahbeyk *et al.* (2017), Silva and Haach (2016) have proposed more appropriate stress-strain models able to reproduce real case, the unified model by Mander *et al.* is still the more widespread and implemented in common structural programs.

The need to improve the seismic performances of existing buildings or to retrofit them according to the new-seismic regulations is a more and more pressing need in areas subjected to high seismic risk (Formisano 2012, Nastri *et al.* 2017, Barbagallo *et al.* 2016). Among the newly available technologies, significant attention has received the confinement of structural members by applying one or more layers of fiber-reinforced materials in a polymeric matrix (FRP) bonded to the element's surface. The increasing use of confinement by FRP requires analytical models able to predict the behavior of confined concrete elements. Many researchers have developed and proposed different constitutive laws. Some of them require an iterative procedure or, as collapse condition, the attainment of the ultimate value of concrete axial strain, while others refer to the ultimate strain of FRP. Some other consider only the maximum amount of the lateral confining, while others its whole development as a function of the concrete axial strain. Generally, these constitutive laws are based on the definition of the confined concrete maximum

strength (f_{cc}) and the corresponding maximum strain (ϵ_{cc}). To estimate the ultimate strength of reinforced concrete elements confined with FRP, several relationships can be found in the literature (Bisby *et al.* 2005, Matthys *et al.* 2005). They are based on the preliminary evaluation of the ultimate lateral confining pressure, and on the assumption that concrete collapse occurs when FRP layers reach their ultimate stress (Karbhari and Gao 1997, Toutanji 1999, Cavaleri *et al.* 2017, Campione 2012, Campione *et al.* 2012, 2014, Saafi *et al.*, 1999, Miyauchi *et al.* 1999, Fadis and Khalili 1981, Spolestra 1999, Xiao and Wu 2000, Motezaker and Kolahchi 2017, Li *et al.* 2017). An extensive comparison of this constitutive models is reported in (Montuori *et al.* 2014a, 2014b) while in this paper reference is made to unreinforced sections only. In the following, among the numerous constitutive models of reinforced confined concrete available in the literature, only the main and widespread ones are reported and detailed. Reference is made to the model by Kent and Park (1971) and the model by Mander *et al.* (1988) which are the ones more implemented in the computer program investigated in the following. Besides, parametric analyses have been led on rectangular column sections with different level of axial load and different stirrups spacing. The accuracy in terms of modelling of the considered structural programs has been investigated by comparing their results with those obtained by applying a theoretical fiber model based on the model by Mander *et al.* (1988).

2. Review of two confined concrete models adopted

2.1 Model by Kent, Park *et al.* (1971-1982)

Kent and Park (1971) presented a piecewise continuous model composed of an ascending parabola and a linear descending branch with a slope that depends on the amount of confinement and finally residual stress of $0,2 f'_c$ where f'_c represent the compressive strength of concrete (Fig. 1). This model does not reflect any strength enhancement due to the confinement steel.

Later modifications by Park, Priestley and Gill (1982) include the effect of confinement upon the strength of concrete. This model assumes a peak strain of 0,002 for unconfined concrete. Starting from Richart *et al.* (1928) linear relationship, Park *et al.* proposed the coefficients to be $k_1=k_2=1$.

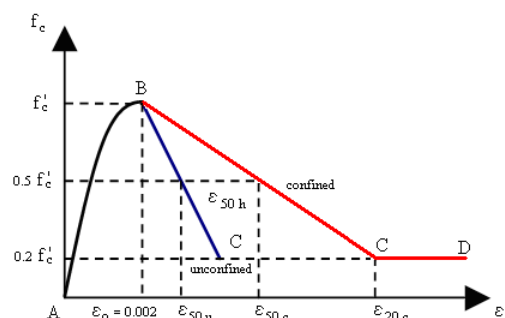


Fig. 1 Model by Kent and Park (1971)

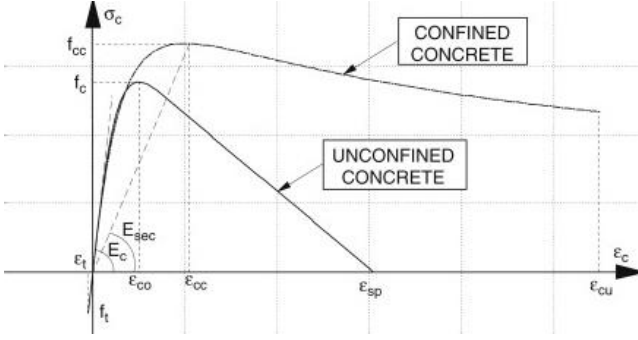


Fig. 2 Stress-Strain Model proposed for monotonic loading of confined and unconfined concrete

$$Richart \text{ et al.} = \begin{cases} f'_{cc} = f'_c + k_1 f_l \\ \varepsilon'_{cc} = \varepsilon'_c \left(1 + k_2 \frac{f_l}{f'_c} \right) \end{cases} \quad (1)$$

where f'_{cc} is the compressive strength of confined concrete, f'_c is the compressive strength of unconfined concrete; f_l is the lateral pressure from the transverse reinforcement; ε'_{cc} is the normal strain corresponding to the maximum stress of the confined concrete, and ε'_c is the normal compressive unconfined concrete strain. The equivalent confining pressure is given by

$$f_l = \rho_s f_{yh} \quad (2)$$

where ρ_s is the ratio of the volume of hoop reinforcement to the volume of confined concrete core measured outside of the hoops, and f_{yh} is the yield strength of the transverse reinforcement.

2.2 Model by Mander, Pristley and Park (1988)

Mander *et al.* (1988) proposed a unified stress-strain approach for confined concrete applicable to both circular and rectangular shaped transverse reinforcement. The stress-strain model is illustrated in Fig. 2 and is based on an equation suggested by Popovics (1973). For a slow (quasi-static) strain rate and monotonic loading, the longitudinal compressive concrete stress f_c is given by

$$f_c = \frac{f'_{cc} r x}{r - 1 + x^r} \quad (3)$$

where f'_{cc} = compressive strength of confined concrete and x is the ratio between the longitudinal compressive concrete strain ε_c and the longitudinal compressive confined concrete strain computed according to the following relationship

$$\varepsilon_{cc} = \varepsilon_{co} \left[1 + 5 \left(\frac{f'_{cc}}{f'_{co}} - 1 \right) \right] \quad (4)$$

as suggested by Richard *et al.* (1928). The terms f'_{co} and ε_{co} are the unconfined concrete strength and corresponding strain, respectively (generally $\varepsilon_{co} = 0,002$ can be assumed), and

$$r = \frac{E_c}{E_c - E_{sec}} \quad (5)$$

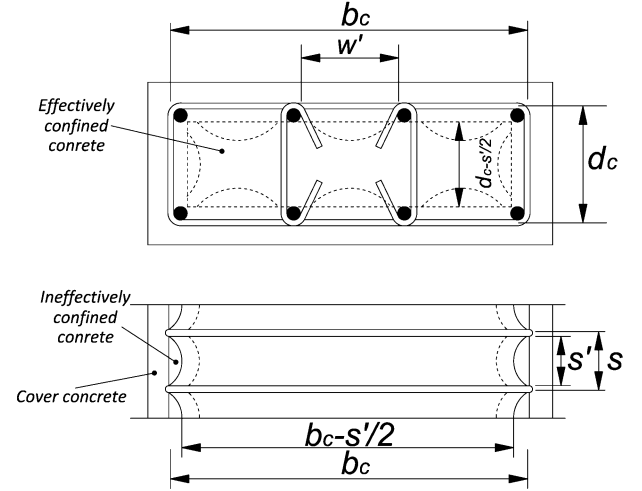


Fig. 3 Effectively confined core for rectangular hoop reinforcement

where the tangent modulus of elasticity of the concrete is expressed as

$$E_c = 5,000 \sqrt{f'_{co}} \text{ MPa} \quad (6)$$

and the secant modulus of elasticity of the concrete is expressed as

$$E_{sec} = \frac{f'_{cc}}{\varepsilon_{cc}} \quad (7)$$

To define the stress-strain behaviour of the cover concrete (outside the confined core concrete) the part of the falling branch in the region where $\varepsilon_c > 2\varepsilon_{co}$ is assumed to be a straight line which reaches zero stress at the spalling strain, ε_{sp} . An approach similar to the one used by Sheikh and Uzumeri (1980) is adopted to determine the effective lateral confining pressure on the concrete section.

The maximum transverse pressure from the confining steel can only be exerted effectively on that part of the concrete core where the confining stress has fully developed due to arching action. Fig. 3 shows the arching action that is assumed to occur between the levels of transverse rectangular hoop reinforcement. The area of ineffectively confined concrete will be largest and the area of effectively confined concrete core A_e will be smallest. It is considered that the effective lateral confining pressure is

$$f'_l = f_l k_e \quad (8)$$

where f_l is lateral pressure from the transverse reinforcement, assumed to be uniformly distributed over the surface of the concrete core, and k_e is the confinement effectiveness coefficient, which is determined by

$$k_e = \frac{A_e}{A_{cc}} \quad (9)$$

where A_e (Equation is the area of effectively confined concrete core; $A_{cc} = A_c(1 - \rho_{cc})$ is the area of concrete core enclosed by the perimeter hoops; A_c is the area of core of section enclosed by the center lines of the perimeter hoop and ρ_{cc} is ratio of area of longitudinal reinforcement

to area of core of section A_c . The arching action is assumed to act in the form of second-degree parabolas with an initial tangent slope of 45° . Arching occurs vertically between layers of transverse hoop bars and horizontally between longitudinal bars. The effectively confined area of concrete at hoop level is found by subtracting the area of the parabolas containing the ineffectively confined concrete. For one parabola, the ineffectual area is $(w'_i)^2/6$ where w'_i is the i th distance between adjacent longitudinal bars. Thus, the total plan area of ineffectually confined core concrete at the level of the hoops when there are n longitudinal bars is

$$A_j = \sum_{i=1}^n \frac{(w'_i)^2}{6} \quad (10)$$

Incorporating the influence of the ineffective areas in elevation, the area of effectively confined concrete core at midway between the levels of transverse hoop reinforcement is

$$A_e = \left(b_c d_c - \sum_{i=1}^n \frac{(w'_i)^2}{6} \right) \left(1 - \frac{s'}{2b_c} \right) \left(1 - \frac{s'}{2d_c} \right) \quad (11)$$

where b_c and d_c are the core dimensions to centre lines of perimeter hoop in x and y directions, respectively, and s' is the vertical spacing between hoops. Hence, the confinement effectiveness coefficient is for rectangular hoops

$$k_e = \frac{\left(1 - \sum_{i=1}^n \frac{(w'_i)^2}{6} \right) \left(1 - \frac{s'}{2b_c} \right) \left(1 - \frac{s'}{2d_c} \right)}{(1 - \rho_{cc})} \quad (12)$$

It is possible for rectangular reinforced concrete members to have different quantities of transverse confining steel in the x and y directions. These may be expressed as

$$\rho_x = \frac{A_{sx}}{s d_c} \quad \text{and} \quad \rho_y = \frac{A_{sy}}{s b_c} \quad (13)$$

where A_{sx} and A_{sy} are the total area of transverse bars running in the x and y directions, respectively, and s is the vertical center to center spacing between hoops. The lateral confining stress on the concrete is given in the x and y directions as

$$f_{lx} = \frac{A_{sx}}{s d_c} f_{yh} = \rho_x f_{yh} \quad (14)$$

$$f_{ly} = \frac{A_{sy}}{s b_c} f_{yh} = \rho_y f_{yh} \quad (15)$$

and f_{yh} is the yield strength of the transverse reinforcement. Therefore, considering the confinement effectiveness coefficient, the effective lateral confining stresses in the x and y directions are

$$f'_{lx} = k_e \rho_x f_{yh} \quad f'_{ly} = k_e \rho_y f_{yh} \quad (16)$$

The evaluation of f'_{cc} (compressive strength of confined concrete) can be performed by means of the

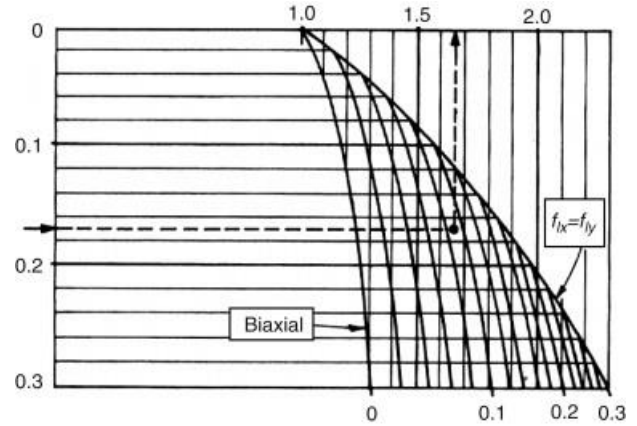


Fig. 4 Confined strength determination from lateral confining stresses for rectangular sections (redrawn from Mander *et al.* 1988)

abacus depicted in Fig. 4, which requires the knowledge of the confining stresses f'_{l1} and f'_{l2} provided by

$$f'_{l1} = \min(f'_{lx}, f'_{ly}) \quad f'_{l2} = \max(f'_{lx}, f'_{ly}) \quad (17)$$

In addition, aiming at a complete description of the constitutive law, it is necessary to determine the ultimate strain ϵ_{cu} which can be estimated employing the following relationship

$$\epsilon_{cu} = 0,004 + \frac{1,4 f_{yh} \rho_s \epsilon_{su}}{f'_{cc}} \quad (18)$$

where ϵ_{su} represents the ultimate steel strain and ρ_s is the volumetric ratio of confining steel which is equal to $\rho_x + \rho_y$. Finally, regarding the tensile strength of concrete, both for confined and unconfined concrete, it is taken as

$$f_t = 0,5 \sqrt{f_{co}} \quad [MPa] \quad (19)$$

The modulus of elasticity in tension is assumed equal to the one in compression.

3. Moment-curvature of reinforced concrete columns

In this work, the moment-curvature of reinforced concrete columns affected by confinement has been provided employing three software: SAP2000, SeismoStruct and Opensees programs which can simulate the inelastic response of structural systems subjected to static loads. Non-linear static analyses on a simple cantilever scheme have been carried out to obtain the plastic response. Results have been compared with those provided by a research software based on a home-made fiber modelling computer program called MCCRCCS (Moment-Curvature Confined Reinforced Concrete Column Sections). MCCRCCS is a software able to provide the moment-curvature diagrams for confined and unconfined concrete for square or rectangular column sections and for sections reinforced with angles and battens.

The philosophy which the fiber hinge model is based on subdivides the cross section of the structural element in

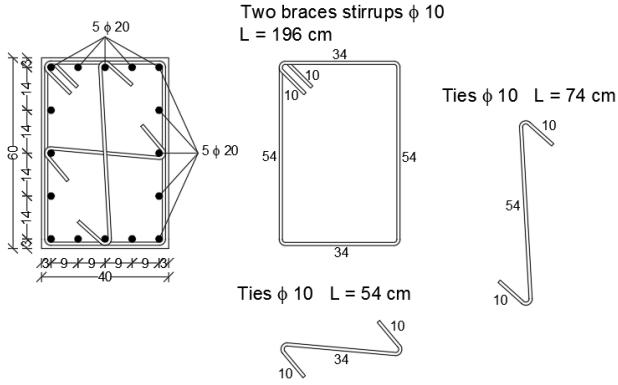


Fig. 5 Cross section of column specimens

Table 1 Mechanical properties of steel and concrete

	Confined Concrete					Unconfined Concrete			Steel	
s [cm]	E_c [MPa]	f_{cc} [MPa]	f_t [MPa]	ϵ_{cc} [-]	ϵ_{cu} [-]	f_{ck} [MPa]	ϵ_{co} [-]	ϵ_{sp} [-]	E_y [MPa]	f_{yk} [MPa]
6	25000	38.375	2.5	0.00735	0.02554					
12	25000	31.375	2.5	0.00455	0.017173	25	0.002	0.01	210000	450
24	25000	27.5	2.5	0.003	0.011514					

three types:

- 1) fibers used for modelling the longitudinal steel reinforcing bars;
- 2) fibers used to define the nonlinear behavior of confined concrete
- 3) fibers used to describe the nonlinear response of unconfined concrete which includes cover concrete.

For each fiber, the stress-strain ($\sigma-\epsilon$) constitutive law is determined.

The geometry, dimensions and reinforcing details of the specimens are shown in Fig. 5. Each sample represents a cantilever column whose length is 3.00 m. The samples have rectangular cross-sections with dimensions $0.40 \times 0.60 \text{ m}^2$. The longitudinal reinforcement of the columns in both lateral faces is composed of sixteen bars of 20 mm diameter. The shear reinforcements in the columns are constituted by 10 mm diameter stirrups spaced at 0.06 m, 0.12 m and 0.24 m. The concrete material is a C25/30, and the reinforcement material is B450C steel.

Table 1 summarizes the mean values of the material properties used in the construction of the samples, where f_{ck} is the cylindrical concrete compressive strength and ϵ_{co} is the corresponding strain; f_{cc} is the compressive strength of confined concrete, and ϵ_{cc} is the corresponding strain; ϵ_{cu} is the ultimate strain; ϵ_{sp} is the concrete spalling strain; f_t is the tensile strength of concrete; E_c is the Young modulus of concrete; f_{yk} is the yield strength of the reinforcement; E_y is the Young modulus of steel. The Eq. (5) proposed by Mander *et al.* (1988) has been applied to define the stress-strain constitutive model of both confined and unconfined concrete according to the mechanical properties reported in Table 1. In Fig. 6 the three constitutive laws referring to confined concrete for the specimens with stirrups spaced at 0.06, 0.12 and 0.24 m and the constitutive law of unconfined concrete are reported. In particular, the distance b_c and d_c are taken to center lines

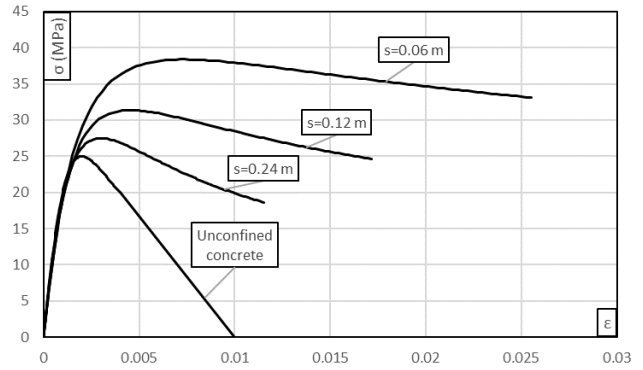


Fig. 6 $\sigma-\epsilon$ constitutive law for concrete with different amounts of horizontal bars

of perimeter hoop in x and y directions as suggested by Mander *et al.* (1988).

In addition, it can be observed that taking the distance b_c and d_c net of the cover concrete, the results concerning stress-strain constitutive law is not affected. Furthermore, 5 level of vertical loads has been applied by considering a percentage of the resistant axial load ($NRd=8136 \text{ kN}$) of the section (Simao *et al.* 2016, Campione *et al.* 2016). The selected percentage are 0% (corresponding to simple bending), 10%, 20%, 30% and 40%. Even if the highest percentage of normalised axial load suggested by Eurocode 8 (CEN 2013) is 65%, it has been decided not to exceed the 40%. For the steel reinforcements, an elastic-perfectly plastic constitutive law has been adopted according to the mechanical properties reported in Table 1.

4. Considered computer programs

4.1 MCCRCCS Research software

Starting from the stress-strain models reported in Fig. 6, a procedure for computing the moment-curvature diagram can be easily outlined by a fiber model. The cross-section has been subdivided into rectangular elementary areas which have been characterized by an appropriate constitutive law: unconfined concrete, confined concrete and steel of the longitudinal reinforcements. To account for the effect of the load acting on the unstrengthened structural member, the deformations occurring in each elementary area before the strengthening intervention must be computed and considered in the subsequent analysis. The different zones of the section, both confined and unconfined, need to be preliminarily recognized. To this aim, the longitudinal confining bars, which are those located in the corners or those out of corners, but restrained by steel ties, must be identified. Starting from these restraining points, it is possible to determine the parabola arches dividing the zones of effectively confined concrete from the zones of unconfined concrete, as it is shown in Fig. 7.

On the bases of the constitutive laws of steel, confined concrete and unconfined concrete, the procedure for evaluating the moment-curvature diagram, for a given axial

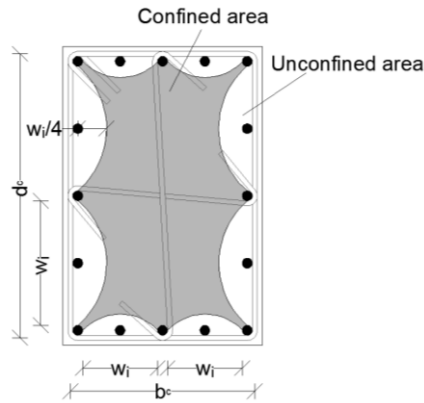


Fig. 7 Identification of confined and unconfined concrete

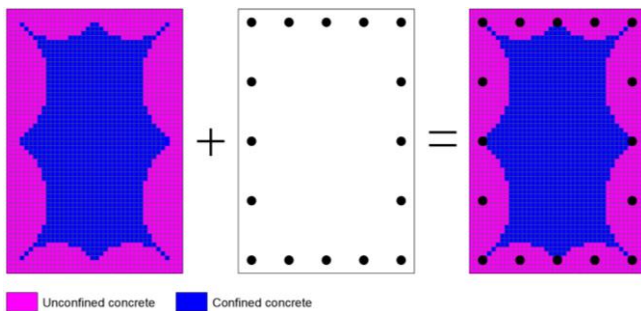


Fig. 8 Fiber subdivision of the cross-section

load has been codified into a computer program namely MCCRCCS. The same code has been used by Montuori and Piluso in previous works (2009, 2015). In particular, Montuori and Piluso made (2009) the validation of the software has been performed on strengthened and unstrengthened R.C. columns showing its accuracy and reliability. The fiber subdivision of the section is reported in Fig. 8. In this case, 40 fibres longitudinally and 60 fibres transversally have been adopted. The areas of steel longitudinal bars have been introduced by their coordinates.

4.2 Sap2000 model

SAP2000 v. 14.0.0 is general-purpose civil-engineering software used for the analysis and design of any structural system (CSI 2007). As regard plastic analysis it allows to account for lumped and spread plasticity using concentrated plastic hinges and fiber hinges whose length can be appropriately selected to capture the actual plastic behavior of the members. In this work, fiber hinge modelling has been exploited by introducing in the software a user-defined fiber section. In particular, the section has been discretized in 60×40 small areas of 1 cm^2 following the same subdivision depicted in Fig. 8 and adopted for the MCCRCCS. For both confined and unconfined concrete, the corresponding stress-strain relationship has been implemented as reported in Fig. 6. Each rebar has been introduced as circular areas and applying a stress-strain relationship of the steel. Concrete materials have been added employing the advanced properties of material ambience accounting for the “Mander” shape of stress-strain behavior already implemented for uniaxial

material typologies.

To provide the moment-curvature of the specimen sections push-over analyses have been carried out on a cantilever scheme whose length is 3 m. The elastic behavior of the member has been simulated using a beam-column element with a $60 \times 40 \text{ cm}^2$ concrete section. To this element, a fiber hinge whose length is equal to the 10% of the global length of the cantilever has been considered. The analyses have been led in displacement control for each level of axial load, taking in account both geometrical and mechanical non-linearities.

4.3 OpenSees models

The Open System for Earthquake Engineering (OpenSees) (Mazzoni *et al.* 2007) is an open source software framework for finite analysis, and it was developed to simulate the response of structural and geotechnical systems subjected to earthquakes. For each considered specimen two nonlinear models were developed using OpenSees computer program, the first one uses Concrete01 model while the second one uses the Concrete04 model.

Uniaxial material Concrete01 is used to construct a uniaxial Kent and Park (1971) with Scott *et al.* (1982) modification concrete material object. Zero tensile strength is accounted for in this model. In addition, a constant residual strength at the crushing strain is considered, so that the material strength in compression is never equal to zero.

Uniaxial material Concrete04 is used to construct a uniaxial concrete material whose envelope of the compressive stress-strain response is defined using the model proposed by Popovics (1973). If the user defines the Young modulus as $E_c = 5,000 \sqrt{f'_{co}}$ then the envelope curve is identical to the one proposed by Mander *et al.* (1988). In this model the compressive stress is equal to zero when the crushing strain is achieved. In addition, it is possible to introduce a tensile stress different to zero. The constitutive laws of Concrete 01 and Concrete 04 are reported in Fig. 9 and Fig. 10, respectively.

The material Steel01 is used to construct a uniaxial bilinear steel material object with kinematic hardening and optional isotropic hardening described by a non-linear evolution equation. It has been used in both the nonlinear model to simulate the stress-strain behaviour of the reinforcing bars. The hardening has been assumed very low (0.0001) to represent an elastic-perfectly plastic behaviour. To provide the moment-curvature of the specimen sections, push-over analyses have been carried out on the same cantilever scheme used in SAP2000. The nonlinear BeamColumn element has been introduced to model the cantilever scheme and it is represented by unidirectional fibres which are assigned by the proper material stress-strain relationships describing the materials monotonic response. It is based on the non-iterative force formulation and considers the spread of plasticity along the element. The section discretization is the same reported in Fig. 8 and it has been introduced by using the “fiber” section command in the software input file. In addition, five integration points were adopted for the column element.

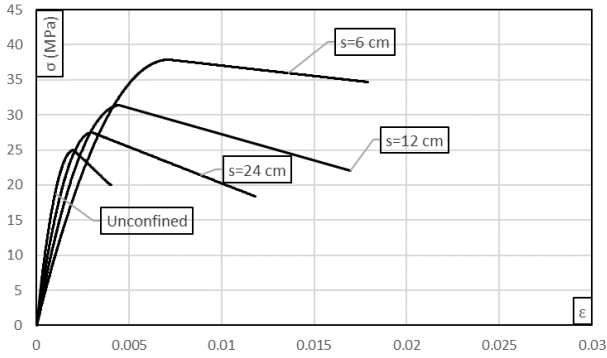


Fig. 9 Constitutive laws of Concrete01

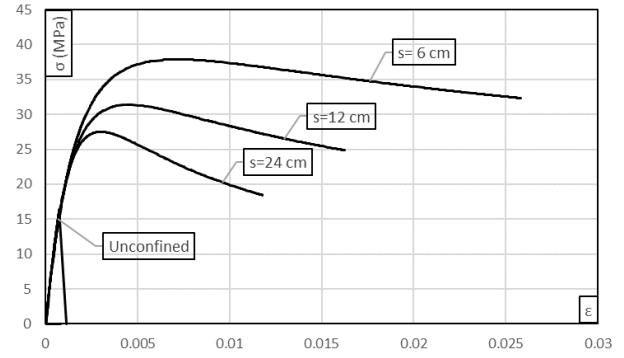


Fig. 10 Constitutive laws of Concrete04

Analysis has been performed in displacement control, so that both geometrical and mechanical non-linear behaviour for each axial load level are accounted for.

4.4 SeismoStruct model

The SeismoStruct 2016 is a finite element package

capable of predicting the large displacements behaviour of space frames under static or dynamic loading, considering geometric nonlinearities and material inelasticity. For each specimen section a nonlinear model was developed. The model was built with inelastic displacement-based frame elements. In SeismoStruct ambient a user-defined fiber section cannot be defined, so that, the material models

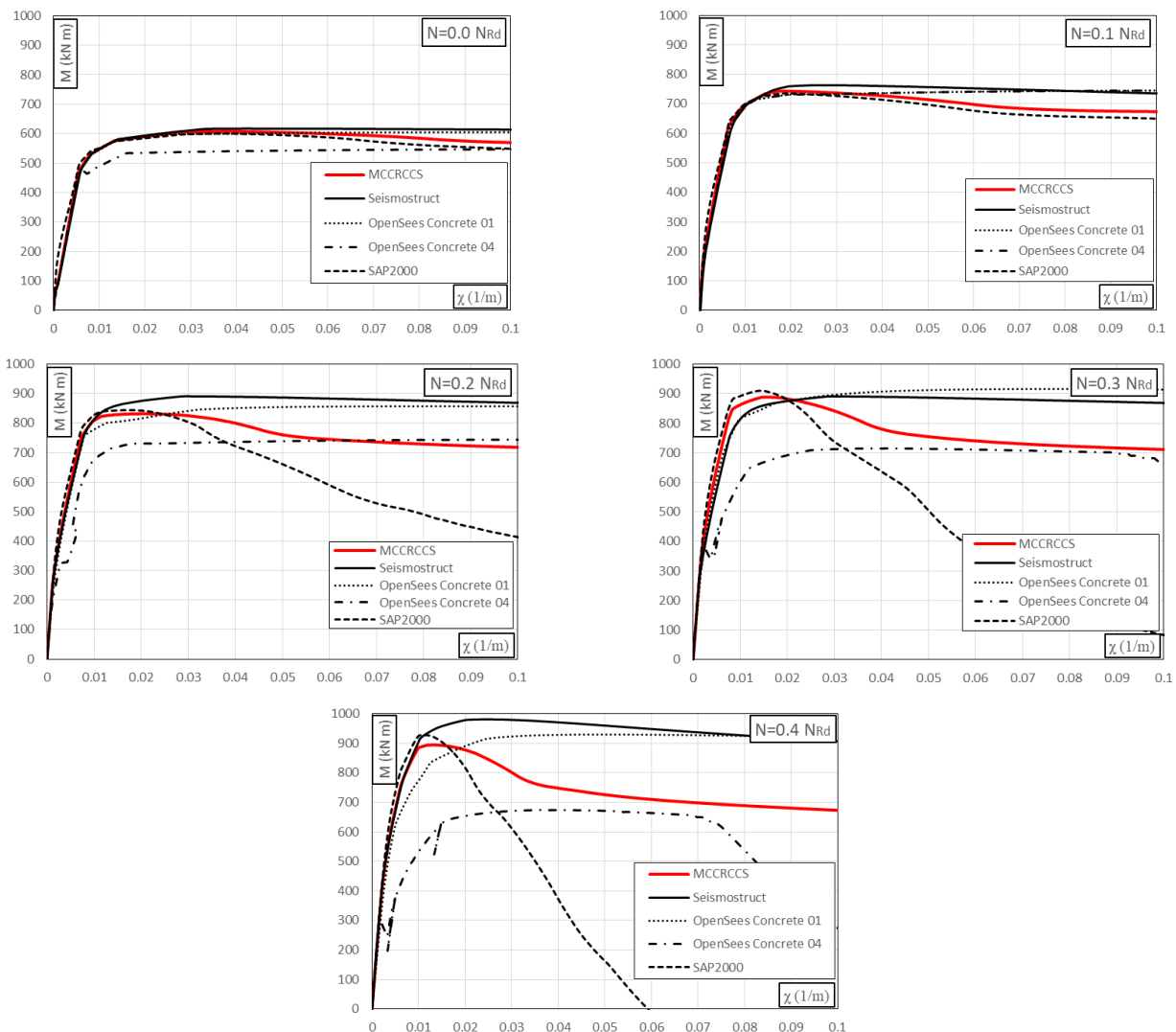


Fig. 11 Moment-Curvature of sections with $s=0.06$ m stirrups spacing

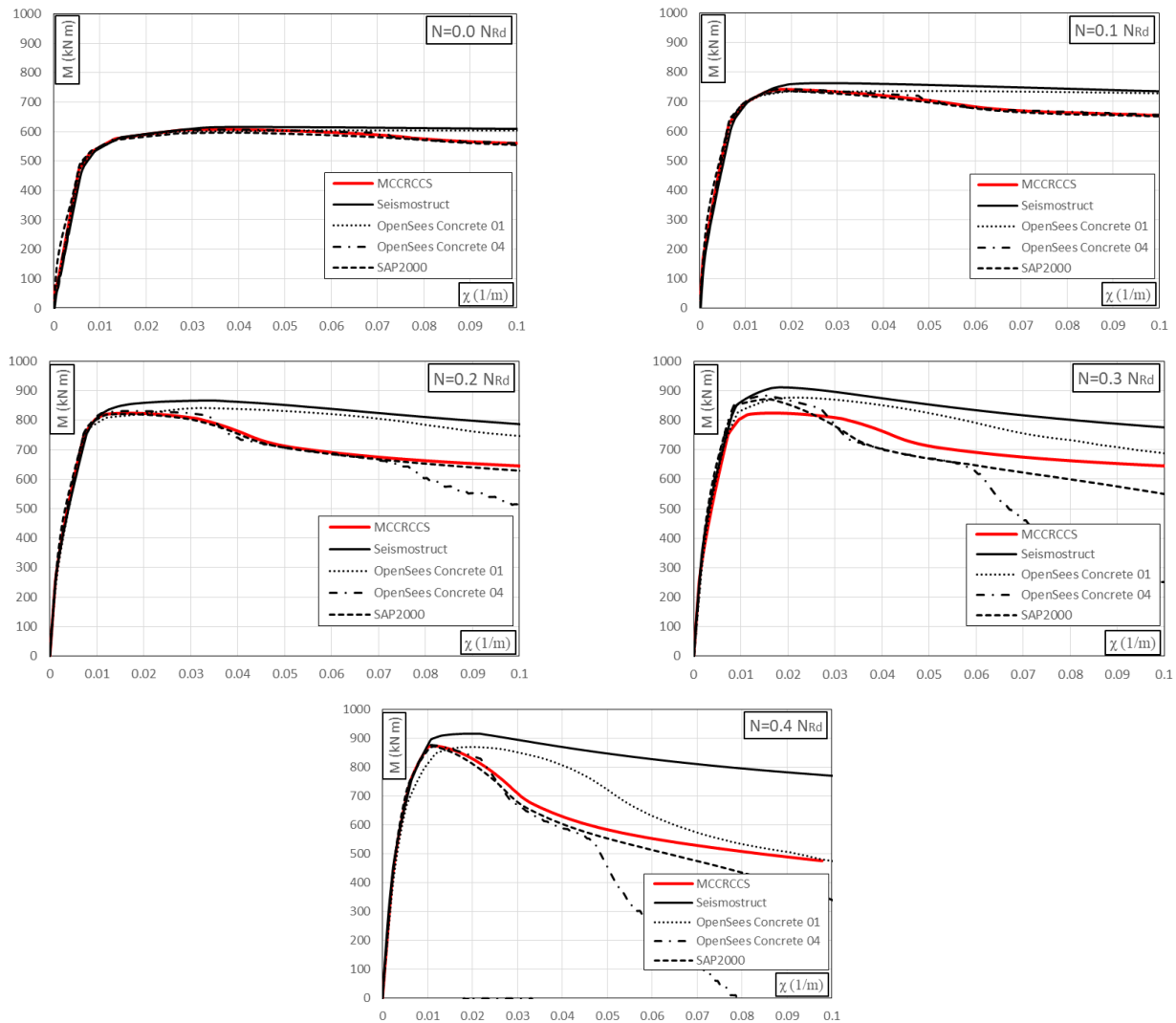


Fig. 12 Moment-Curvature of sections with $s=0.12$ m stirrups spacing

“con_ma” (Mander *et al.* 1988) has been adopted for both the confined and unconfined concrete. This is a uniaxial nonlinear constant confinement model that follows the constitutive relationship proposed by Mander *et al.* (1988). The confinement effects provided by the lateral transverse reinforcements are incorporated through the rules proposed by Mander *et al.* whereby constant confining pressure is assumed through the entire stress-strain range.

The effectiveness of the SeismoStruct modelling has been preliminarily validated by checking the confinement ratio parameter (f'_{cc}/f'_c) provided by the software with the one extracted by the abaqus reported in Fig. 4. In the case of unconfined concrete, a confinement ratio equal to 1 has automatically assumed by the software. In addition, “stl_bl” is adopted for the reinforcement bars with a very low hardening parameter to simulate an elastic-perfectly plastic behaviour (0.0001). The section has been discretized into 1000 fibers (the maximum number of fibers available in the software). To provide the moment-curvature of the specimen sections, a push-over analyses have been carried out on the same cantilever scheme used in SAP2000 discretized in 4 parts for each level of axial load.

5. Results

Besides the calculation of a moment-curvature ($M-\chi$) diagram the aim of the work is to highlight how the different software modelling affects the shape of $M-\chi$ diagram. In Fig. 11, Fig. 12, and Fig. 13 the moment-curvature diagrams of the section with the stirrups spacing of 0.06 m, 0.12 m and 0.24 m are reported, respectively. In addition, in the same figures the moment-curvature diagrams are reported with reference to different levels of the axial load. In a first comparison it is possible to observe that the curves representative of SAP2000 are more in accord with the curve representative of MCCRCCS on average. In particular, SAP2000 is able to well catch the resistance but it is not always able to reproduce the softening branch of the research program. From the SeismoStruct side, it is possible to observe that the resistance is well captured by the software but for increasing levels of the axial load the SeismoStruct overestimate the resistance.

The OpenSees computer program provides $M-\chi$ diagram significantly different in the case of the Concrete01

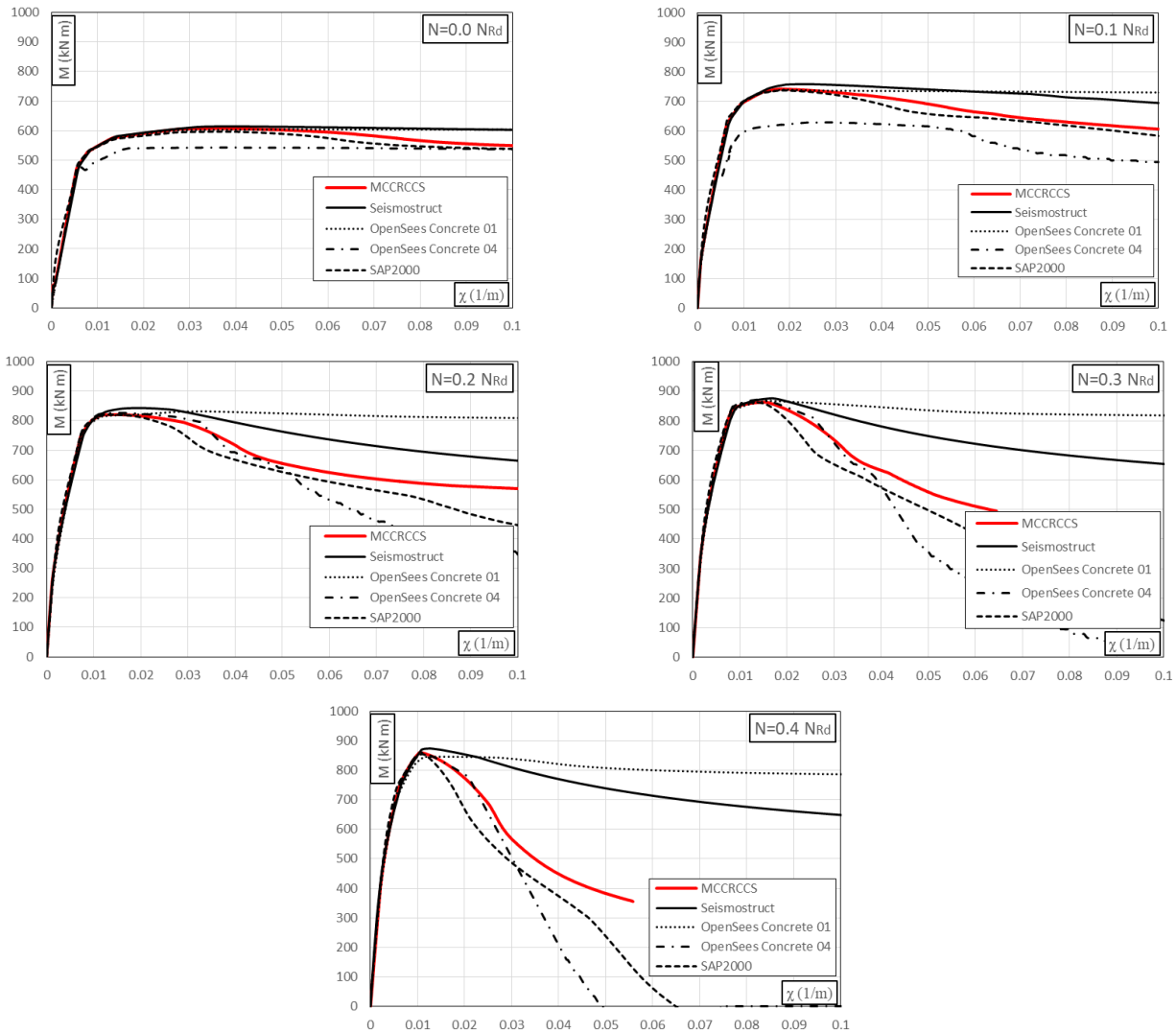


Fig. 13 Moment-Curvature of sections with $s=0.24$ m stirrups spacing

and Concrete04 uniaxial material. Concrete04 model, in the largest part of cases, underestimate the resistance while the Concrete01 shows moment-curvature diagrams closer to the SeismoStruct ones. Finally, the softening branch of the SeismoStruct and Concrete01 $M-\chi$ diagrams are always higher than those provided by the other models. It is observed that the resistance is well captured by the largest part of the software with the only exclusion of the Concrete04 model. In addition, the results between the curves became more different as the axial load increase. As regards the differences in terms of moment-curvature between the section with different stirrups spacing, it can be noted that varying the spacing of stirrups from 0.06 m to 0.24 m there is no substantial difference in the comparison between the results of MCCRCCS and the other four models considered.

In Fig. 14 the moment-curvature diagrams are reported also with reference to OpenSees only for a value of N equal to $0.1 N_{Rd}$ and a stirrup spacing equal to 0.12 m. In particular, the black lines refer to the discretization described in Fig. 8 of the present work. Conversely, the magenta lines refer to different OpenSees modelling that is

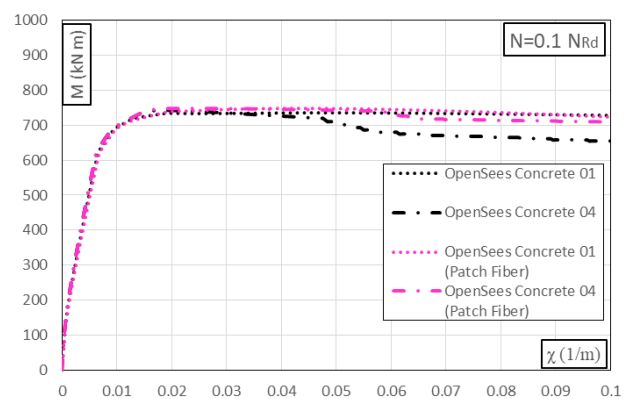


Fig. 14 Moment-Curvature of sections with $s=0.12$ m stirrups spacing - comparison between OpenSees models

the one suggested by the software manual. In particular, the fiber section discretization is made by means of the “patch” command that allows to reproduce square or rectangular fiber sections. In this case, the section is divided into an external patch representative of the section cover, a rectangular inner patch representative of the core concrete

and the steel rebars. Unconfined concrete is assigned to the external patch of the cover while confined concrete is assigned to the inner patch of the core concrete. Such kind of modelling is not able to capture the effectively confined concrete area, i.e., it is not able to automatically select the area of parabolas that must be considered as unconfined concrete. In fact, from Fig. 14 the magenta lines, are higher than the black lines. This is due to the overestimation of the confined concrete area that belongs to considering all the concrete core as confined. Therefore, the use of this model can lead to an overestimation of the reinforced concrete section and does not constitute an improvement in the description of section behavior.

5. Conclusions

In this work, a comparison among the most diffused structural programs such as Sap2000, OpenSees and SeismoStruct in terms of moment-curvature ($M-\chi$) of R.C. columns are reported. The results obtained by this software have been compared with those provided by a “home-made” computer program, namely MCCRCCS, used as benchmark result. This program accuracy has been validated against strengthened and unstrengthened R.C. columns showing its accuracy and reliability (Montuori and Piluso 2009). The calculation of a moment-curvature ($M-\chi$) shows that the curves representative of SAP2000 are, on average, more in accord with the curve representative of MCCRCCS with respect to the other two software. Regarding the SeismoStruct and the OpenSees with Concrete01 material, it can be observed that the resistance is overestimate and for increasing levels of the axial load this overestimation increases. In addition, for high values of curvature the overestimation became unacceptable. Furthermore, the OpenSees computer program provides $M-\chi$ diagram significantly different depending on the uniaxial material model adopted for concrete. In particular, the use of concrete 04 model can lead results which are very far from the actual ones. Regarding moment-curvature between the section with different stirrups spacing, there is no substantial difference between the results of MCCRCCS and the other four models considered. Finally, regarding the OpenSees modelling, the use of the so-called “patch” command, suggested by the manual, instead of the subdivision of the section according to the effectively confined areas, does not provide any actual improvement in the description of moment curvature diagram.

References

- Ahmad, S.M. and Shah, S.P. (1982), “Stress-strain curves of concrete confined by spiral reinforcement”, *J. Proc.*, **79**(6), 484-490.
- Ahmad, S.M. and Shah, S.P. (1985), “Behavior of hoop confined concrete under high strain rates”, *J. Proc.*, **82**(5), 634-647.
- Balmer, G.G. (1944), “Shearing strength of concrete under high triaxial stress-computation of Mohr's envelope as a curve”, SP-23, Structural Research, Laboratory, U.S. Bureau of Reclamation.
- Barbagallo, F., Bosco, M., Marino, E.M., Rossi, P.P. and Stramondo, P.R. (2016), “Seismic upgrading of vertically irregular existing R.C. frames by BRBs”, *Geotech. Geolog. Earthq. Eng.*, **40**, 181-192.
- Bisby Luke, A., Dent Aaron, J.S. and Green Mark, F. (2005), “Comparison of confinement models for fiber-reinforced polymer-wrapped concrete”, *ACI Struct. J.*, 102-S07.
- Campione, G. (2012), “Flexural behavior of steel fibrous reinforced concrete deep beams”, *J. Struct. Eng.*, **138**(2), 235-246.
- Campione, G., Cavaleri, L., Di Trapani, F., Macaluso, G. and Scaduto, G. (2016), “Biaxial deformation and ductility domains for engineered rectangular RC cross-sections: A parametric study highlighting the positive roles of axial load, geometry and materials”, *Eng. Struct.*, **107**, 116-134. <https://doi.org/10.1016/j.engstruct.2015.10.030>.
- Campione, G., Fossetti, M., Giacchino, C. and Minafò, G. (2014), “RC columns externally strengthened with RC jackets”, *Mater. Struct./Mater. Constr.*, **47**(10), 1715-1728. <https://doi.org/10.1617/s11527-013-0146-x>.
- Campione, G., Fossetti, M., Minafò, G. and Papia, M. (2012), “Influence of steel reinforcements on the behavior of compressed high strength R.C. circular columns”, *Eng. Struct.*, **34**, 371-382. <https://doi.org/10.1016/j.engstruct.2011.10.002>.
- Cavaleri, L., Di Trapani, F., Ferrotto, M.F. and Davì, L. (2017), “Stress-strain models for normal and high strength confined concrete: Test and comparison of literature models reliability in reproducing experimental results”, *Ingegneria Sismica*, **34**, 114-137.
- Cavaleri, L., Di Trapani, F., Ferrotto, M.F. and Davì, L. (2017), “Stress-strain models for normal and high strength confined concrete: Test and comparison of literature models reliability in reproducing experimental results”, *Ingegneria Sismica*, **34**(3-4), 114-137.
- Chang, G.A. and Mander, J.B. (1994), “Seismic energy based fatigue damage analysis of bridge columns: Part 1-evaluation of seismic capacity”, Technical Report, March.
- CSI SAP 2000 (2007), “Integrated finite element analysis and design of structures”, Analysis Reference, Computer and Structure Inc., University of California, Berkeley.
- Cusson, D. and Paultre, P. (1995), “Stress-strain model for confined high-strength concrete”, *J. Struct. Eng.*, **121**(3), 468-477.
- Cusson, D., De Larrard, F., Boulay, C. and Paultre, P. (1996), “Strain localization in confined high-strength concrete columns”, *J. Struct. Eng.*, **122**(9), 1055-1061.
- Desayi, P., Iyengar, K.T.S.A. and Reddy, T.S. (1978), “Equations for stress-strain curve of concrete confined in circular steel spiral”, *Mater. Struct. Res. Test.*, **11**(65), 339-345.
- Dhakar, R.P. and Maekawa, K. (2002), “Modeling for postyield buckling of reinforcement”, *J. Struct. Eng.*, **128**(9), 1139-1147.
- Dilger, W.H., Koch, R. and Kowalczyk, R. (1984), “Ductility of plain and confined concrete under different strain rates”, *J. Proc.*, **81**(1), 73-81.
- Fardis, M.N. and Khalili, H. (1981), “Concrete encased in fibre glass-reinforced plastic”, *ACI Mater. J.*, **78**(5), 440-446.
- Formisano, A. (2012), “Seismic damage assessment of school buildings after 2012 Emilia Romagna earthquake”, *Ingegneria Sismica*, **29**(2-3), 72-86.
- Karbhari, V.M. and Gao, Y. (1997), “Composite jacketed concrete under uniaxial compression-verification of simple design equations”, *J. Mater. Civil Eng.*, ASCE, **9**(4), 185-192. [https://doi.org/10.1061/\(ASCE\)0899-1561\(1997\)9:4\(185\)](https://doi.org/10.1061/(ASCE)0899-1561(1997)9:4(185)).
- Kent, D.C. and Park, R. (1971), “Flexural members with confined concrete”, *J. Struct. Div.*, ASCE, **97**(7), 1969-1990.
- Li, L.J., Zeng, L., Xu, S.D. and Guo, Y.C. (2017), “Experimental study on axial compressive behavior of hybrid FRP confined

- concrete columns”, *Comput. Concrete*, **19**(4), 395-404. <https://doi.org/10.12989/cac.2017.19.4.395>.
- Mander, J.B., Priestley, M.J.N. and Park, R. (1988), “Theoretical stress-strain model for confined concrete”, *J. Struct. Eng.*, ASCE, **114**(8), 1804-1826. [https://doi.org/10.1061/\(ASCE\)0733-9445\(1988\)114:8\(1804\)](https://doi.org/10.1061/(ASCE)0733-9445(1988)114:8(1804)).
- Matthys, S., Toutanji, H., Audenaert, K. and Taerwe, L. (2005), “Axial load behavior of largescale columns confined with fiber-reinforced polymer composites”, *ACI Struct. J.*, **102**(2), 258- 265.
- Mazzoni, S., McKenna, F., Scott, M.H. and Fenves, G.L. (2007), “OpenSees command language manual”, Pacific Earthquake Engineering Research Center, University of California, Berkeley, U.S.A.
- Miyauchi, K., Inoue, S., Kuroda, T. and Kobayashi, A. (1999), “Strengthening effects of concrete columns with carbon fiber sheet”, *Tran. JPN Concrete Inst.*, **21**, 143-150.
- Montuori, R. and Piluso, V. (2009), “Reinforced concrete columns strengthened with angles and battens subjected to eccentric load”, *Eng. Struct.*, **31**, 539-550. <https://doi.org/10.1016/j.engstruct.2008.10.005>.
- Montuori, R. and Piluso, V. (2015), “Analysis and modelling of CFT members: Moment curvature analysis”, *Thin Wall. Struct.*, **86**, 157-166. <https://doi.org/10.1016/j.tws.2014.10.010>.
- Montuori, R., Piluso, V. and Tisi, A. (2012a), “Comparative analysis and critical issues of the main constitutive laws for concrete elements confined with FRP”, *Compos. Part B*, **43**, 3219-3230. <https://doi.org/10.1016/j.compositesb.2012.04.001>.
- Montuori, R., Piluso, V. and Tisi, A. (2012b), “Ultimate behaviour of FRP wrapped sections under axial force and bending: Influence of stress-strain confinement model”, *Compos. Part B: Eng.*, **54**(1), 85-96. <https://doi.org/10.1016/j.compositesb.2013.04.059>.
- Motezaker, M. and Kolahchi, R. (2017), “Seismic response of concrete columns with nanofiber reinforced polymer layer”, *Comput. Concrete*, **20**(3), 361-368. <https://doi.org/10.12989/cac.2017.20.3.361>.
- Nastri, E., Vergato, M. and Latour, M. (2017), “Performance evaluation of a seismic retrofitted R.C. precast industrial building”, *Earthq. Struct.*, **12**(1), 13-21. <https://doi.org/10.12989/eas.2017.12.1.013>.
- Park, R. and Leslie, P.D. (1977), “Curvature ductility of circular reinforced concrete columns confined by the ACI spiral”, *6th Australasian Conf. on the Mech. of Struct. and Mater.*, **1**, 342-349.
- Park, R., Priestley, M.J.N. and Gill, W.D. (1982), “Ductility of square-confined concrete columns”, *J. Struct. Div.*, ASCE, **108**(4), 929-950.
- Popovics, S. (1973), “A numerical approach to the complete stress-strain curves for concrete”, *Cement Concrete Res.*, **3**(5), 583-599. [https://doi.org/10.1016/0008-8846\(73\)90096-3](https://doi.org/10.1016/0008-8846(73)90096-3).
- Razvi, S. and Saatcioglu, M. (1999), “Confinement model for high-strength concrete”, *J. Struct. Eng.*, **125**(3), 281-289. [https://doi.org/10.1061/\(ASCE\)0733-9445\(1999\)125:3\(281\)](https://doi.org/10.1061/(ASCE)0733-9445(1999)125:3(281)).
- Richart, F.E., Bradtzaeg, A. and Brown, R.L. (1928), “A study of the failure of concrete under combined compressive stresses”, Bulletin No. 185, Engineering experimental station University of Illinois, Urbana, USA.
- Richart, F.E., Brandtzaeg, A. and Brown, R.L. (1929), “The failure of plain and spirally reinforced concrete in compression”, Bulletin 190, Univ. of Illinois Engineering Experimental Station, Champaign, 111.
- Roy, H.E.H. and Sozen, M.A. (1964), “Ductility of concrete”, *Proc. Int. Symp. on the Flexural Mech. of Reinforced Concrete*, ASCE-American Concrete Institute, 213-224.
- Saafi, M., Toutanji, H.A. and Li, Z. (1999), “Behavior of concrete columns confined with fiber reinforced polymer tubes”, *ACI Mater. J.*, **96**(4), 500-509.
- Scott, B.D., Park, R. and Priestley, M.J.N. (1982), “Stress-strain behavior of concrete confined by overlapping hoops at low and high strain rates”, *J. Proc.*, **79**(1), 13-27.
- SeismoStruct (2016), available on http://www.seismosoft.com/SeismoStruct_2016_Release-5_ITA
- Shahbeyk, S., Moghaddam, M.Z. and Safarnejad, M. (2017), “A physically consistent stress-strain model for actively confined concrete”, *Comput. Concrete*, **20**(1), 85-97. <https://doi.org/10.12989/cac.2017.20.1.085>.
- Sheikh, S.A. and Uzumeri, S.M. (1980), “Strength and ductility of tied concrete columns”, *J. Struct. Div.*, ASCE, **106**(5), 1079-1102.
- Sheikh, S.A. and Uzumeri, S.M. (1982), “Analytical Model for concrete confinement in tied columns”, *J. Struct. Div.*, ASCE, **108**, 2703-2722.
- Silva, M.F.A. and Haach, V.G. (2016), “Parametrical study of the behavior of exterior unreinforced concrete beam-column joints through numerical modeling”, *Comput. Concrete*, **18**(2), 215-233. <https://doi.org/10.12989/cac.2016.18.2.215>.
- Simão, P.D., Barros, H., Ferreira, C.C. and Marques, T. (2016), “Closed-form moment-curvature relations for reinforced concrete cross-sections under bending moment and axial force”, *Eng. Struct.*, **129**, 67-80. <https://doi.org/10.1016/j.engstruct.2016.09.033>.
- Spoolstra, M.R. and Monti, G. (1999), “FRP-confined concrete model”, *J. Compos. Constr.*, ASCE, **3**(3), 143-150. [https://doi.org/10.1061/\(ASCE\)1090-0268\(1999\)3:3\(143\)](https://doi.org/10.1061/(ASCE)1090-0268(1999)3:3(143)).
- Toutanji, H.A. (1999), “Stress-strain characteristics of concrete columns externally confined with advanced fiber composite sheets”, *ACI Mater. J.*, **96**(3), 397-405.
- UNI EN 1998-1 (2013), Eurocode 8-Design of Structures for Earthquake Resistance - Part 1: General Rules, Seismic Actions and Rules For Buildings.
- Vellenas, J., Bertero, V.V. and Popov, E.P. (1977), “Concrete confined by rectangular hoops subjected to axial loads”, Report 77/13, Earthquake Engineering Research Center, Univ. of California, Berkeley, Calif.
- Xiao, Y. and Wu, H. (2000), “Compressive behavior of concrete confined by carbon fiber composite jackets”, *J. Mater. Civil Eng.*, ASCE, **12**(2), 139-146. [https://doi.org/10.1061/\(ASCE\)0899-1561\(2000\)12:2\(139\)](https://doi.org/10.1061/(ASCE)0899-1561(2000)12:2(139)).

CC